

Water Resources Research®

RESEARCH ARTICLE

10.1029/2023WR035126

Key Points:

- Recession limb groundwater proportion is a strong predictor of summer low flows
- Recession limb dynamics are especially important for improving low-flow prediction at rain-dominated sites
- Recession limb groundwater may be a better predictor of low flow at sites where dynamic storage exceeds deep storage

Supporting Information:

Supporting Information may be found in the online version of this article.

Correspondence to:

K. Johnson and P. L. Sullivan,
johnkeir@oregonstate.edu;
pamela.sullivan@oregonstate.edu

Citation:

Johnson, K., Harpold, A., Carroll, R. W. H., Barnard, H., Raleigh, M. S., Segura, C., et al. (2023). Leveraging groundwater dynamics to improve predictions of summer low-flow discharges. *Water Resources Research*, 59, e2023WR035126. <https://doi.org/10.1029/2023WR035126>

Received 4 MAY 2023

Accepted 12 JUL 2023

Author Contributions:

Conceptualization: Keira Johnson, Adrian Harpold, Rosemary W. H. Carroll, Holly Barnard, Pamela L. Sullivan

Data curation: Keira Johnson, Adrian Harpold, Rosemary W. H. Carroll, Mark S. Raleigh, Wenming Dong

Formal analysis: Keira Johnson, Rosemary W. H. Carroll, Catalina Segura, Wenming Dong, Pamela L. Sullivan

Funding acquisition: Holly Barnard, Li Li, Kenneth H. Williams, Pamela L. Sullivan

Investigation: Keira Johnson

Methodology: Keira Johnson, Adrian Harpold, Rosemary W. H. Carroll, Holly Barnard, Mark S. Raleigh, Catalina Segura, Pamela L. Sullivan

Project Administration: Pamela L. Sullivan

© 2023. American Geophysical Union.
All Rights Reserved.

Leveraging Groundwater Dynamics to Improve Predictions of Summer Low-Flow Discharges

Keira Johnson¹, Adrian Harpold² , Rosemary W. H. Carroll³ , Holly Barnard⁴ , Mark S. Raleigh¹ , Catalina Segura⁵ , Li Li⁶ , Kenneth H. Williams^{7,8} , Wenming Dong⁷ , and Pamela L. Sullivan¹ 

¹College of Earth, Ocean and Atmospheric Science, Oregon State University, Corvallis, OR, USA, ²Department of Natural Resources and Environmental Science, University of Nevada, Reno, NV, USA, ³Division of Hydrologic Sciences, Desert Research Institute, Reno, NV, USA, ⁴Department of Geography, Institute of Arctic and Alpine Research, University of Colorado Boulder, Boulder, CO, USA, ⁵Forest Engineering Resources and Management, College of Forestry, Oregon State University, Corvallis, OR, USA, ⁶Department of Civil and Environmental Engineering, Pennsylvania State University, State College, PA, USA, ⁷Lawrence Berkeley National Laboratory, Berkeley, CA, USA, ⁸Rocky Mountain Biological Lab, Gothic, CO, USA

Abstract Summer streamflow predictions are critical for managing water resources; however, warming-induced shifts from snow to rain regimes impact low-flow predictive models. Additionally, reductions in snowpack drive earlier peak flows and lower summer flows across the western United States increasing reliance on groundwater for maintaining summer streamflow. However, it remains poorly understood how groundwater contributions vary interannually. We quantify recession limb groundwater (RLGW), defined as the proportional groundwater contribution to the stream during the period between peak stream flow and low flow, to predict summer low flows across three diverse western US watersheds. We ask (a) how do snow and rain dynamics influence interannual variations of RLGW contributions and summer low flows?; (b) which watershed attributes impact the effectiveness of RLGW as a predictor of summer low flows? Linear models reveal that RLGW is a strong predictor of low flows across all sites and drastically improves low-flow prediction compared to snow metrics at a rain-dominated site. Results suggest that strength of RLGW control on summer low flows may be mediated by subsurface storage. Subsurface storage can be divided into dynamic (i.e., variability saturated) and deep (i.e., permanently saturated) components, and we hypothesize that interannual variability in dynamic storage contribution to streamflow drives RLGW variability. In systems with a higher proportion of dynamic storage, RLGW is a better predictor of summer low flow because the stream is more responsive to dynamic storage contributions compared to deep-storage-dominated systems. Overall, including RLGW improved low-flow prediction across diverse watersheds.

Plain Language Summary Water managers across the western United States depend on accurate streamflow prediction models for water planning and allocation during summer months. Historically, these models use snow metrics to predict summer flows, but increasing temperatures across the western US are decreasing snow input and accumulation and increasing early snow melt rates leading to changes in streamflow generation mechanisms. Here, we seek to understand how stream flows will respond under warmer climates in three watersheds with distinct climate and underlying bedrock in the western US. We expanded upon commonly used low-flow model snow metrics to include snow and streamflow metrics from the previous year as well as groundwater dynamics during the annual recession curve. We found that including variables outside of commonly used snow parameters in the models produced more accurate predictions of summer low flows. We provide a framework for future analysis of streamflow response to warming across the western US.

1. Introduction

Current climate models predict that surface air temperatures will warm as a result of increasing concentrations of greenhouse gases in the atmosphere (IPCC, 2022). In snow- and ice-dominated regions, these increasing temperatures are concomitant with decreases in snow accumulation due to a shift in precipitation phase from snow to rain (Berghuis et al., 2014; Feng & Hu, 2007) and increases in snow melt rate during the mid-to-late snow season (Harpold & Brooks, 2018; Kapnick & Hall, 2012; Mote et al., 2018; Musselman et al., 2021). In snow-dominated watersheds, earlier snowpack melt has resulted in earlier peak flows in streams and lower summer low flows

Resources: Pamela L. Sullivan
Supervision: Pamela L. Sullivan
Validation: Keira Johnson, Mark S. Raleigh
Visualization: Keira Johnson, Holly Barnard, Pamela L. Sullivan
Writing – original draft: Keira Johnson, Pamela L. Sullivan
Writing – review & editing: Keira Johnson, Adrian Harpold, Rosemary W. H. Carroll, Holly Barnard, Mark S. Raleigh, Catalina Segura, Li Li, Kenneth H. Williams, Pamela L. Sullivan

(e.g., Azmat et al., 2017; Bavay et al., 2009; Carroll et al., 2018; Kapnick & Hall, 2012; Milly & Dunne, 2020; Poyck et al., 2011; Segura et al., 2019; I. T. Stewart et al., 2005). However, the response of summer low flow in systems undergoing changes in precipitation regimes remains equivocal (e.g., Godsey et al., 2014; Huntington & Niswonger, 2012; Mayer & Naman, 2011; Segura et al., 2019). Understanding the response of low flows to changing climate conditions can benefit managers around the world (Brooks et al., 2021; Floriancic et al., 2021; Godsey et al., 2014; Gordon et al., 2022; Svensson & Prudhomme, 2005). Therefore, we focus on summer low flows, a period when high-water demand by both human and non-human users coincide and requires accurate predictions of water availability.

Many processes play a role in summer streamflow generation in the western, montane United States, beginning with snow accumulation and mid-winter snow dynamics (Musselman et al., 2021) through the onset of snowmelt (Barnhart et al., 2016), infiltration, and subsurface transport of meltwater (Gordon et al., 2022). Predictions of summer low-flow dynamics in these regions have relied heavily on incorporating winter snow metrics (e.g., peak snow water equivalent (SWE), melt rate, and snowfall fraction) into models (Godsey et al., 2014; Tague & Grant, 2009), while groundwater dynamics are rarely leveraged. We focus on quantifying groundwater contributions to the stream between peak streamflow and summer low flow (i.e., the falling limb of the stream hydrograph following the snowmelt pulse) because this period dictates the quantity of meltwater and precipitation that recharges groundwater, regulates water residence times, and governs the interaction between shallow and deep flow paths (Kapnick & Hall, 2012). This period denotes the annual recession limb, and we term the groundwater contribution to the stream during this period as recession limb groundwater (RLGW).

End member mixing analysis (EMMA) can quantify the contribution of groundwater to streamflow and illuminate the proportion of RLGW contributed to a stream and its relationship to summer low flows. EMMA uses naturally occurring environmental tracers, such as stable isotopes of water and conservative constituents, with distinct chemical signatures (e.g., Cl, Ca, and Na) among sources (e.g., rain, snow, unsaturated groundwater, shallow groundwater, and deep groundwater) in conjunction with stream discharge to approximate the proportional amount of each source contributing to the streamflow (Carroll et al., 2018; Cowie et al., 2017; Hooper, 2003; Miller et al., 2014; Segura et al., 2019). Geogenic constituents that exhibit negative concentration–discharge ($C-Q$) relationships can be leveraged to understand groundwater–surface water interactions (Bernal et al., 2006; Genereux et al., 1993; B. Stewart et al., 2022) as these species indicate higher groundwater contributions during low flows and lower groundwater contributions during high flows. In streams with strong negative $C-Q$ relationships, EMMA provides a flexible yet robust method for quantifying groundwater contribution to streamflow across different years and environments.

The behavior of RLGW inputs into streams and its relationship to summer low flow likely vary depending on the dominant type of winter precipitation (i.e., snow/transition/rain) and the proportion of dynamic versus deep groundwater storage. Evidence from snow-dominated systems with a large proportion of deep groundwater storage, indicated by long mean residence times, show that summer low flows are more sensitive to inter-annual than the intra-annual precipitation inputs (Brooks et al., 2021; Godsey et al., 2014). In contrast, summer low flows in rain-dominated and transition basins, especially those with small deep groundwater reservoirs, are more responsive to same year precipitation dynamics (Safeeq et al., 2013). In systems across the western US, summer streamflows are sustained by groundwater, but the age differs depending on the proportion of dynamic to deep storage within each system (Godsey et al., 2014; Huntington & Niswonger, 2012; Rademacher et al., 2005; Tague & Grant, 2004). Stream water composition during spring snowmelt is less consistent than summer flows and has been shown to be influenced by snowmelt rate (Barnhart et al., 2016), vegetation, topography, and drought (Carroll et al., 2018). Based on these findings, we propose using the variable nature of stream chemistry during the recession limb to understand RLGW inputs. We hypothesize that recession limb stream chemistry will provide insight into groundwater dynamics before summer low flow that lead to better predictions of summer low-flow discharge compared to snow metrics alone. Predictive power will be greater in transition/rain-dominated catchments, where summer low flows are less coupled with snow melt.

To test our hypothesis and improve understanding of summer low-flow dynamics, we focus on two questions: (a) how do snow and rain dynamics influence interannual variation of RLGW proportion and summer flow volume?; and (b) what watershed attributes impact the effectiveness of RLGW as a predictor of summer low-flow volume? To address these questions, we examined historic streamflow and climate data from three watersheds that vary in climate and lithology. For the low-flow analyses, we focus on the lowest fifth percentile flow, termed

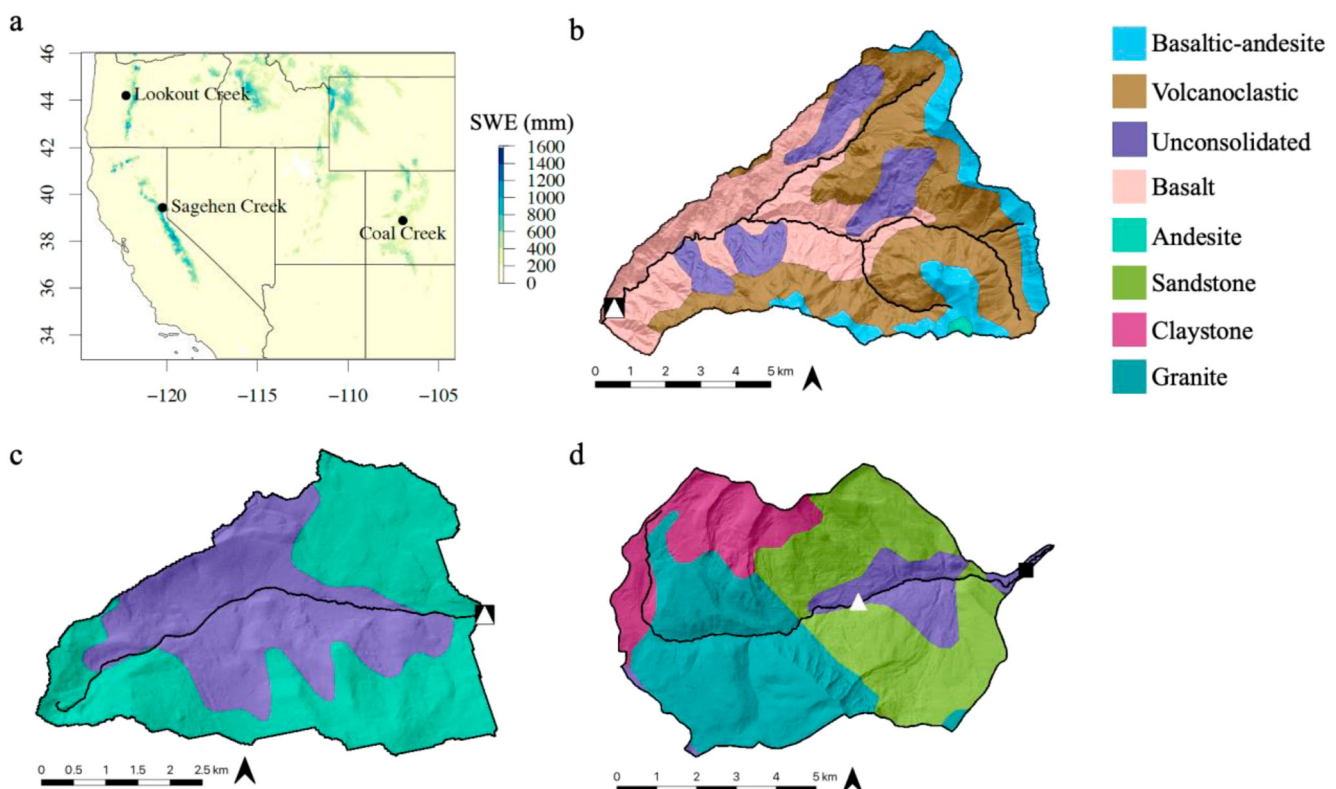


Figure 1. Location of each watershed (a) with colors indicating average 1 April snow water equivalent (SWE) between 2004 and 2020 from Snow Data Assimilation System (SNODAS) across the western US. Individual watershed maps of Lookout Creek (b), Sagehen Creek (c), and Coal Creek (d). The black line indicates the mainstem of each creek. The white triangle is the location where the chemistry data are collected, and the black square is the US Geological Survey (USGS) gage associated with each stream. Background colors represent the underlying lithology sourced from State Geologic Map Compilation (Horton et al., 2017).

Q_5 (sometimes referred to as Q_{95} ; Smakhtin, 2001), as it is a commonly used metric to represent low-flow conditions and has been shown to be vulnerable to warming (Carlier et al., 2018; Laaha & Blöschl, 2005; Meresa et al., 2022; Smakhtin, 2001; Wang & Cai, 2009), more so than Q_{10} (Dinpashoh et al., 2019).

2. Methods

2.1. Study Sites

Three unregulated streams that vary in lithology and climatic regime were selected to investigate the relationship among snow dynamics, RLGW contributions, and summer stream water low flows (Figure 1 and Table 1). Lookout Creek (64 km^2) is a tributary to the Blue River and located on the western side of the Oregon Cascades within the HJ Andrews Experimental Forest. Sagehen Creek (27 km^2) is a tributary to Stampede Reservoir located on the eastern side of the Central Sierra Nevada north of Truckee, CA. Coal Creek (53 km^2) is a tributary to the Slate River in the Central Rocky Mountains.

Lookout Creek receives the most annual precipitation of the three watersheds with an average of 1,453 mm year $^{-1}$, with $>80\%$ falling between November and April (Jones & Perkins, 2010), predominantly as rain. Above 800 m, snowpack generally persists from November through June; however, at lower elevations snowpack rarely lasts for more than 2 weeks. In comparison, Sagehen Creek and Coal Creek receive an average precipitation of 1,065 and 1,147 mm year $^{-1}$, respectively. Like Lookout Creek, Sagehen Creek receives most of its precipitation in the winter and annually about 60% falls as snow. In contrast, Coal Creek receives about 75% of its precipitation as snow and the remaining falls as rain in the summer during the North American monsoon season. Despite the variation in snow inputs across the watersheds, snow plays an important role in streamflow generation at all three sites.

All three basins were shaped by glacial erosion, and glacial till is present along the stream channel. Lookout Creek is underlain by volcanic rocks that vary with elevation. Below 760 m, hydrothermally altered Oligocene to

Table 1
Basin Characteristics at Lookout, Sagehen, and Coal Creeks

Parameter	Lookout Creek	Sagehen Creek	Coal Creek
Elevation (m)	410–1,630	1,755–2,658	2,712–3,688
Size (km ²)	64	27	53
Average Q (m ³ /s)	3.3	0.3	0.8
Average low flow (m ³ /s) ^a	0.26	0.05	0.07
Annual air temperature (°C)	8	6	1
Annual precipitation (mm) ^b	1,453	1,065	1,147
Snowfall fraction ^b	0.11	0.62	0.74
Underlying geology	Volcanic	Volcanic/granitic	Granitic/sedimentary
Underlying soils	Loam	Sandy/gravelly loam	Loamy-skeletal
Dominant vegetation	Conifer	Conifer	Conifer (north aspect), deciduous (south aspect)

Note. Details on years used to calculate average hydrologic metrics can be found in Table S1 in Supporting Information S1.

^aLow flow defined as fifth percentile flow, constrained to between August 1 and October 31. ^bEstimated from Snow Data Assimilation System (SNODAS).

early-Miocene age breccias and tuffs from mudflows and pyroclastic flows dominate. Between 760 and 1,200 m, bedrock is composed of Miocene age ash flows and basalt and andesite flows, and above 1,200 m, Pliocene to early-Miocene andesite flows make up the bedrock. Generally, these formations are highly weathered and fractured because of hydrothermal alteration and cooling and shrinking of flow material (Swanson & James, 1975). The lower elevations of Lookout Creek are prone to debris flows in response to large storms and enhanced by roads and clearcutting. Sagehen Creek is underlain by Cretaceous granites and granodiorites, which are overlain by Miocene and Pleistocene andesitic volcanic flows, breccias, and basalts. Granodiorite outcrops are found in the northwest portion of the basin, while andesitic outcrops are found at high elevations within the watershed (Rademacher et al., 2005). Coal Creek watershed is the only one with any significant sedimentary bedrock; the lower Coal Creek watershed is underlain predominately by the late Cretaceous Mesaverde formation sandstone. The upper portion of the watershed is underlain by intrusive plutonic rock, originating during the Middle Tertiary. Areas of the upper north slope of the watershed are underlain by Wasatch Formation mudstone (Gaskill, 1991).

2.2. Data Products

2.2.1. Stream Water Discharge and Chemistry

Continuous stream discharge is available for all three sites from the United States Geological Survey (USGS; Table S1 in Supporting Information S1). Coal Creek discharge is directly measured during ice-free periods (15 April 15 to 15 November), but the USGS gage is removed during winter. Coal Creek continues to flow beneath the ice and therefore a regression was developed to estimate discharge during winter periods using a downstream gage on the Slate River (USGS Site ID 385106106571000, Text S1 in Supporting Information S1). Stream chemistry was retrieved from different locations for each site (Table S1 in Supporting Information S1).

2.2.2. Snow Data Assimilation System Data Product

The Snow Data Assimilation System (SNODAS) is a daily, 1 km² resolution modeled snow product available for the contiguous US from National Oceanic and Atmospheric Administration (NOAA) National Weather Service's National Operational Hydrologic Remote Sensing Center (NOHRSC, 2004). SNODAS estimates snow parameters (e.g., snow cover, SWE, and sublimation) using a spatially distributed energy and mass balance snow model. Daily SWE and liquid precipitation data from water year 2004 through 2020 were downloaded from the NSIDC archive using the *rwrhydro* package (McCreight et al., 2015) and clipped to the watershed area delineated using the USGS spatial analysis tool StreamStats. Daily watershed SWE was calculated by summing daily SWE across each grid cell within the watershed to get a total watershed SWE for each day. Watershed peak SWE was calculated using highest daily cumulative watershed peak SWE for a given water year and dividing it by the watershed area. Liquid precipitation was calculated by summing liquid precipitation across all grid cells for all days within each water year and dividing the total watershed liquid precipitation by the watershed area. From these data, the

Table 2

SNODAS Parameters, Their Definitions, and the Mean and Standard Deviation of Each Parameter at Each Watershed From Water Years 2004–2020

Parameter (units)	Definition	Lookout Creek	Sagehen Creek	Coal Creek
Peak SWE (mm)	Maximum amount of snow accumulation for a given water year	159 ± 108	666 ± 337	861 ± 306
SWE lag (mm)	Previous water year's peak SWE	154 ± 110	681 ± 342	853 ± 315
Peak SWE day (SWD) (WY day)	Day of the water year that peak SWE occurs	138 ± 35	172 ± 30	194 ± 24
Snow disappearance day (SDD) (WY day)	Day of the water year that the snowpack disappears permanently	232 ± 37	286 ± 24	271 ± 18
Melt rate (mm/day)	Rate of snow disappearance (peak SWE/SDD – PSD)	1.6 ± 0.8	6.0 ± 2.8	11.8 ± 4.2
Total precipitation (mm)	Total amount of precipitation received over the course of a given water year	1,453 ± 407	1,065 ± 459	1,147 ± 270
Liquid precipitation (mm)	Total rainfall amount received over the course of a given water year	1,294 ± 374	398 ± 231	286 ± 146
Snowfall fraction	Proportion of precipitation that falls as snow (peak SWE/total precipitation)	0.11 ± 0.07	0.62 ± 0.18	0.74 ± 0.13

parameters in Table 2 were calculated. SNODAS SWE data were validated against Airborne Snow Observatory (ASO) lidar surveys (Painter et al., 2016) that occurred at Sagehen Creek and Coal Creek during the period of study (Text S2 in Supporting Information S1).

2.3. Estimation of Groundwater Contribution and Summer Low Flow

To quantify groundwater contributions to streamflow, we used chemical hydrograph separation (CHS). CHS is considered to have a more physical basis than graphical hydrograph separation since it incorporates hydrochemical information (Foks et al., 2019), leading to a more accurate estimation of baseflow in snow-dominated environments (Miller et al., 2014). It relies on mass balance and uses stream discharge and the chemical signature of source waters to separate components of a hydrograph (Hooper, 2003). CHS assumes that stream water is a mix of fixed composition source solutions, and the mixing processes of these source solutions are linear (Barthold et al., 2011). To select the best solutes to represent these end members, we used a concentration–discharge (C – Q) analysis approach. CHS relies on robust log linear C – Q relationships. C – Q relationships of geogenic solutes were examined across all three sites and the constituent with the highest average log linear R^2 was used.

Estimating groundwater contributions on daily time steps required deriving continuous concentrations based on discrete concentration measurements and continuous flow data. Given that sampling frequency of stream water chemistry varied across the watersheds from daily to monthly, the Weighted Regressions on Time, Discharge, and Season (WRTDS) from the EGRET R package was used (Hirsch et al., 2010, 2023). The WRTDS model is a USGS analysis method to predict daily stream chemistry designed to allow for more flexibility than a basic regression model by using a shifting C – Q relationship among seasons, over time, and across the hydrograph. The general formula of the model is

$$E[c] = w(Q, T) \quad (1)$$

where c is concentration, $E[c]$ is predicted concentration, and w is a function that depends on discharge (Q) and time (T). The WRTDS model was run for the length of the overlapping discrete chemical and continuous discharge records, and continuous chemical data were estimated for each site at a daily time step. The WRTDS model provides a flux bias statistic which indicates how well the model fits the measured fluxes (product of c and Q , kg/day) and is defined as the difference between the sum of the estimated fluxes on all sampled days and the sum of the true fluxes on all sampled days. A bias statistic near zero indicates low bias in the model, and values above/below ±0.1 (unitless) indicate that the model is highly biased and should not be used for that data set. A Nash–Sutcliffe efficiency (NSE) value was also calculated for each site to evaluate the goodness of fit between observed and modeled stream chemistry values (Nash & Sutcliffe, 1970). NSE was calculated using the hydroGOF R package (Zambrano-Bigiarini, 2020).

CHS was run using the modeled daily stream chemistry and measured daily stream discharge. CHS assumes that all stream water is a combination of two broad end members: groundwater and runoff (i.e., surface runoff,

interflow, and shallow groundwater flow). We used the established approach of estimating end member concentrations from stream chemistry during high and low flows (Kish et al., 2010; Miller et al., 2014; M. Stewart et al., 2007). This approach relies on a strong C – Q relationship but eliminates the need for measured runoff and groundwater chemistry to represent an end member. In our case, C – Q relationships showed a strong log linear dilution pattern (average R^2 of 0.80; Figure S4 in Supporting Information S1). During high flows when the stream discharge peaks and the stream constituent concentration is at its lowest, the stream is assumed to be composed of 100% runoff (Kish et al., 2010; Miller et al., 2014; M. Stewart et al., 2007). Here, runoff does not represent direct rainwater or snowmelt inputs but rather these inputs after picking up solutes on their way into the stream (Miller et al., 2014). For this reason, our runoff end members are more geochemically evolved than rainwater or snowpack.

During low flows when the stream discharge is at its lowest and the stream constituent concentration peaks, the stream is assumed to be composed of 100% groundwater. In this sense, runoff is defined as water with a low chemical concentration and groundwater as water with a high chemical concentration. Using these definitions, the following equation was used to calculate the volume of streamflow made up of groundwater:

$$Q_{BF} = Q \left[\frac{C - C_{RO}}{C_{BF} - C_{RO}} \right] \quad (2)$$

where Q_{BF} is daily mean groundwater discharge, Q is daily mean discharge, C is the daily mean stream concentration, C_{RO} is the concentration of the runoff end member, and C_{BF} is the concentration of the baseflow end member. When groundwater and runoff chemistry are unavailable, end members can be estimated using the upper/lower limit measured constituent concentrations: C_{RO} can be estimated as the lowest measured constituent concentration and C_{BF} as the highest measured constituent concentration (Kish et al., 2010; Miller et al., 2014; Rumsey et al., 2015; M. Stewart et al., 2007). Consistent end member values assume that the end members are temporally consistent. As shown by Miller et al. (2014) and Rumsey et al. (2015), this assumption is valid for C_{RO} because the temporal variation in snow melt and rain is small relative to the instream constituent concentrations. This assumption is not valid for C_{BF} because groundwater constituent concentrations vary based on residence time, which may vary year to year. Therefore, C_{BF} concentrations were calculated for each year. Four combinations of possible end members can be used in CHS (Miller et al., 2014): two that represent runoff inputs and two that represent groundwater inputs. For runoff end members, either the minimum or the first percentile of end member solute concentrations can be used. For groundwater end members, either the maximum or the 99th percentile of end member solute concentrations can be used. In general, 99th and 1st percentiles are more representative of average runoff and groundwater conditions and therefore are used (Miller et al., 2014). End members were calculated from observed, not modeled, concentrations. Our analysis began with all four combinations and the final section was based on combinations where only positive groundwater inputs were estimated.

RLGW proportion was calculated by averaging the modeled groundwater proportion from the CHS across the recession limb. At each site, the recession limb was identified as the months encompassing the falling limb of the hydrograph after peak SWE to minimum streamflow (Figure 2). Summer low-flow discharge was calculated using the fifth percentile flow discharge and is referred to as $Q5$. $Q5$ calculation was constrained to only consider the fifth percentile flow that occurred between 1 August and 31 October such that winter low flow at Coal Creek would not be included.

2.4. Statistical Analyses

2.4.1. Principal Components Analysis

Principal components analysis (PCA) was used to assess drivers of RLGW and $Q5$ and identify potential multicollinearity between variables. Climate parameters (Table 2), RLGW, $Q5$, and lagged $Q5$ and RLGW for all three sites were included in the PCA. Data were centered and scaled to achieve normal distribution, and PCA was run using R package *PCAtools* (Blighe & Lun, 2022). PCs above the elbow of the scree plot were retained. Significance of each parameter on each PC was tested using a 99% confidence interval *t* test. Parameters that were not significant on any retained PC were removed from subsequent analysis. Where eigenvectors were collinear, the one with the largest eigenvalue was retained, and others were removed from subsequent analysis.

2.4.2. Multiple Linear Regression

Multiple linear regression models were used to investigate the relationships among snow parameters (Table 2), low-flow discharge, and RLGW proportion. In addition to the snow and rain variables included in Table 2, $Q5$ lag,

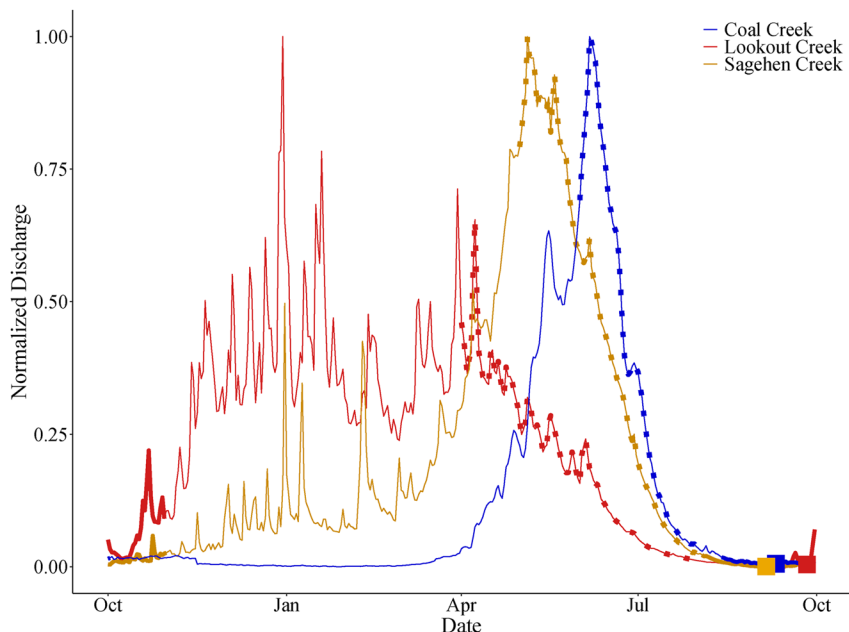


Figure 2. Minimum–maximum normalized average annual water year stream discharge for watersheds for Lookout (red), Sagehen (yellow), and Coal (blue) Creeks. Dotted portion of the hydrographs indicate recession limb. Bold portions of the hydrograph indicate the range during which low flow occurred over the period of record. Colored square indicates mean low-flow date.

defined as the previous year's summer low-flow discharge, and RLGWlag, defined as the previous year's RLGW, were included as predictor variables. PCA was used to determine which parameters would be used in the models to reduce multicollinearity and overfitting. Coal Creek only has 5 years of data; therefore, time lags were not investigated. Best models were determined using backward stepwise Akaike information criterion (AIC) model selection from the *MASS* R package (Venables & Ripley, 2002) on center and scaled data to achieve normal distribution. Once best models were determined, multicollinearity was checked using a variance inflation factor (VIF). Variables with a $VIF > 10$ were removed and models were checked again. This was repeated until all retained variables had a VIF less than 10. Regression/beta coefficients were calculated to evaluate relative importance of each retained variable on model output using the *QuantPsc* R package (Fletcher, 2022).

2.4.3. Leave-One-Out-Cross-Validation

Leave-one-out-cross-validation (LOOCV) was used to assess model performance (Stone, 1974). LOOCV splits a data set into a training set and a testing set but leaves only one data point for the testing set. A model is built using the training set and uses the model to predict the response variable of the training data. This process is repeated n times, where n is the number of observations in the data set. LOOCV is often used for validation of models built with small data sets because it does not require extensive training and testing data. LOOCV was run on each model using the *MuMIn* R package (Barton, 2023) for each site and the RMSE of the original model was compared to the mean of the RMSE from the LOOCV test runs.

3. Results

3.1. SNODAS–ASO Comparison

We evaluated SNODAS data with measured lidar snow depth and estimated SWE from ASO surveys. SNODAS and ASO data were compared on one survey at Sagehen Creek (26 March 2016) and two surveys at Coal Creek (30 March 2018, 7 April 2019); ASO data were not available at Lookout Creek. The Sagehen Creek flight was an average snow year (Figure S1 in Supporting Information S1), while the Coal Creek flights sampled a low (2018) and high (2019) snow year (Figures S2 and S3 in Supporting Information S1). In general, SNODAS overpredicted SWE at low elevations and underpredicted at high elevations compared to ASO. Average watershed SWE

differences between SNODAS and ASO from all three flights ranged from 0.13% to 12.74%, indicating SNODAS slightly overpredicts watershed average SWE (Text S2 in Supporting Information [S1](#)).

3.2. Characterization of SWE and Stream Hydrographs

Hydrograph response reflects the timing of rainfall and snow melt of each site (Figure 2). Lookout Creek had the smallest snowfall fraction (0.11) and the earliest average peak SWE of the three sites (early February; Table 2). Lookout Creek also had the greatest interannual variability in snow accumulation and peak SWE, with peak SWE occurring as early as December or as late as March. Sagehen Creek and Coal Creek had later and more consistent peak SWE that tended to fall in late March and mid-April, respectively. Sagehen Creek and Coal Creek had the highest snowfall fraction 0.62 and 0.74, respectively (Table 2). Lookout Creek generally reached peak flow in mid-winter (i.e., December–January) due to fall and winter precipitation, reflecting its rain-dominated nature. Peak flow at Sagehen and Coal Creeks was later than Lookout Creek and characteristic of snow-dominated sites, with peaks occurring in late April and mid June, respectively. Fall and winter rain at Sagehen Creek and Lookout Creek caused large peaks in the hydrograph prior to the snowmelt pulse. After snowmelt, flow in all three streams decreased and reached baseflow by August.

3.3. End Member Mixing Analysis

$C-Q$ behavior of geogenic solutes was examined across the three sites to select a solute that would be used in the WRTDS model and for CHS. The slopes of the $C-Q$ relationships were negative for all tested geogenic solutes. At all sites, sodium, magnesium, and calcium showed the strongest $C-Q$ relationship (R^2 ranged from 0.41 to 0.95; Figure S4 in Supporting Information [S1](#)). Calcium was selected for the WRTDS and CHS models as it demonstrated a strong log linear relationship with discharge (average R^2 of 0.80) and was the best fit at Lookout Creek which had weakest $C-Q$ relationships of the three sites (Figure S4 in Supporting Information [S1](#)).

The WRTDS model was run across time periods where discrete calcium and continuous discharge records were available. In general, WRTDS accurately predicted calcium concentrations, with the best predictions at moderate flows (Figure S5 in Supporting Information [S1](#)). Models at all three sites had low bias statistics and high NSE (range 0.84–0.95). Calcium and discharge generally covaried (Figure S5 in Supporting Information [S1](#)) where high flows were associated with low calcium values and low flows were associated with high calcium values. Lookout Creek calcium values had a lower seasonal range, with average minimum and maximum concentrations differing by less than 2 mg/L, compared to a seasonal range of about 10 mg/L at Sagehen and Coal Creeks.

At all three sites, the 99th percentile calcium concentration was selected as the best groundwater end member for CHS because these values are more representative of groundwater concentrations than the maximum calcium concentration (Miller et al., 2014). For Lookout Creek and Coal Creek, the first percentile calcium concentrations were selected for the runoff end member using the same reasoning. At Sagehen Creek, the minimum calcium concentration was used as the runoff end member as the first percentile calcium concentration resulted in a model that predicted negative baseflow volumes. On average, Sagehen Creek had the highest weighted groundwater contribution throughout the year (41%) and Coal Creek had the lowest groundwater contribution throughout the year (24%).

Groundwater contribution varied throughout the year and across years, but generally contributed higher proportions during low flow periods and lower proportions during high flow periods (Figure 3). Minimum groundwater contributions ranged from 5% at Coal Creek to 21% at Lookout Creek. These minimum contributions occurred during early March, mid-April, and early May at Lookout, Sagehen, and Coal Creeks, respectively. As expected because of diluting log-linear $C-Q$ relationships across all three streams, the maximum groundwater contribution occurred in mid-to-late August across all three sites when flows were at their lowest. However, higher contributions of baseflow were also estimated at Lookout and Sagehen Creeks following fall and winter storms, likely due to flushing of high concentrations of constituents stored in the soils from the first rains after long, dry summers (Rademacher et al., 2005; Vanderbilt et al., 2003). During the spring snowmelt pulse, groundwater contributions were low at Sagehen and Coal Creeks, which indicated that runoff and water transport through the shallow subsurface from snowmelt was the dominant contribution to the stream. Groundwater contribution also varied across years, suggesting that groundwater dynamics are responsive to interannual variations in precipitation. Average annual weighted minimum proportional groundwater contributions occurred in 2005 at Lookout Creek

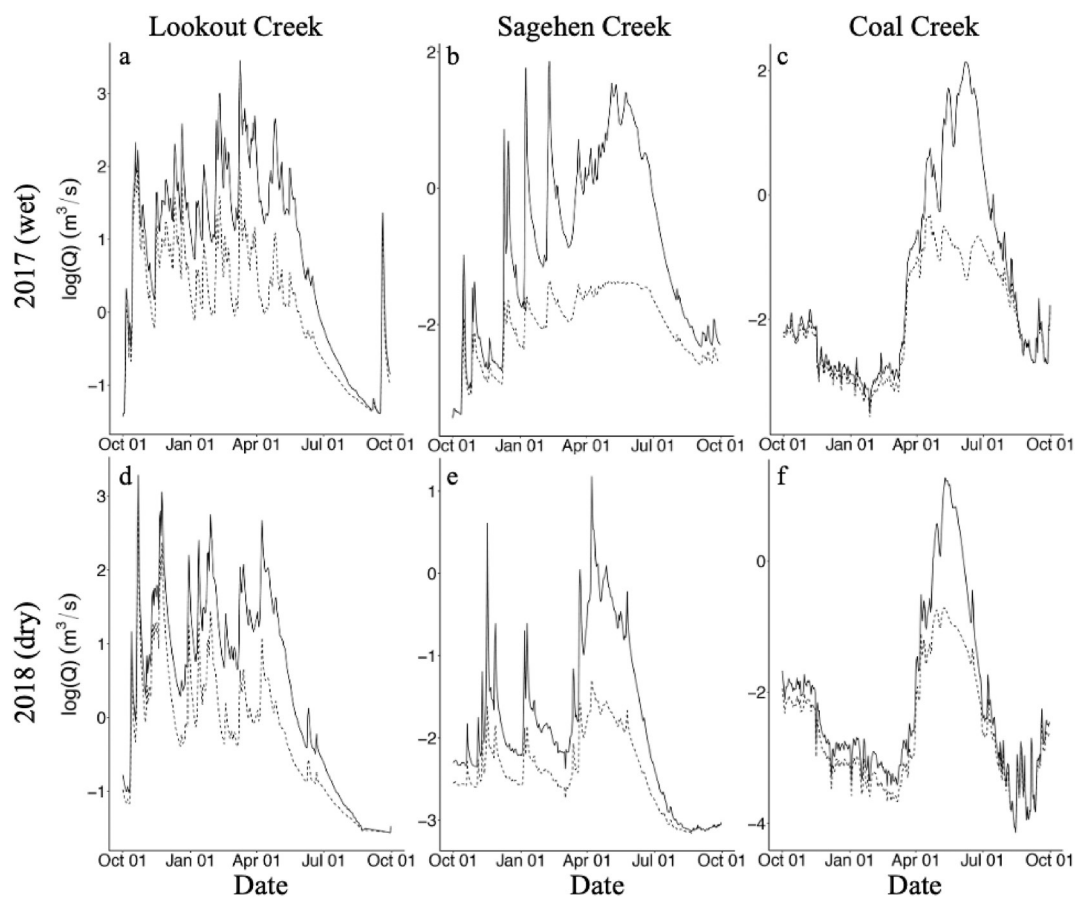


Figure 3. Chemical hydrograph separation for 2017 (top) and 2018 (bottom) for (a, d) Lookout Creek, (b, e) Sagehen Creek, and (c, f) Coal Creek. Solid lines represent the total flow and dashed lines represent the groundwater contribution.

(31%), in 2017 at Sagehen Creek (17%; Figure 3b), and in 2019 at Coal Creek (17%). Average annual maximum proportional groundwater contributions occurred in 2013 at Lookout Creek (42%), in 2015 at Sagehen Creek (64%), and in 2018 at Coal Creek (33%; Figure 3f).

RLGW proportions varied across sites, reflecting variation in hydrologic regime and streamflow generation processes. All sites had average RLGW proportions between 0.4 and 0.5. Average values were highest at Sagehen Creek (0.48) and lowest at Coal Creek (0.41). RLGW proportion generally covaried with peak SWE (Figure 4a).

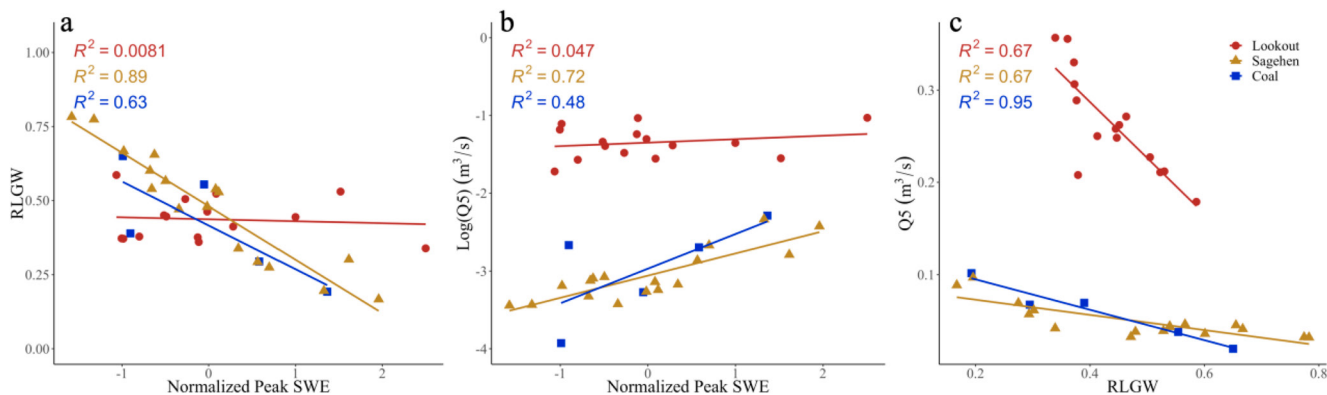


Figure 4. Linear relationships between annual (a) recession limb groundwater (RLGW) and z-score normalized peak snow water equivalent (SWE), (b) $\log Q5$ and z-score normalized peak SWE, and (c) $Q5$ and RLGW for Lookout Creek (red circle), Sagehen Creek (yellow triangle), and Coal Creek (blue square).

Years with higher peak SWE had lower RLGW proportions and years with lower peak SWE had higher RLGW proportion. RLGW proportion was significantly correlated to peak SWE at Sagehen Creek ($R^2 = 0.89, p < 0.01$) and strongly correlated at Coal Creek ($R^2 = 0.63, p = 0.11$) but not significantly correlated at Lookout Creek. Sites where RLGW proportion was more related to peak SWE had higher interannual variability; the lowest interannual variability was observed at Lookout Creek ($CV = 0.16$) and the highest values observed at Sagehen Creek ($CV = 0.40$) and Coal Creek ($CV = 0.45$).

3.4. Low-Flow Discharge

Onset of low flow varied across the sites. The earliest and latest occurrence of $Q5$ occurred at Sagehen Creek on 3 August and 31 October, respectively. At Lookout Creek, $Q5$ occurred between 24 August and 30 October, and at Coal Creek $Q5$ occurred between 13 August and 2 October. Mean $Q5$ dates were earliest at Sagehen Creek (5 September) and latest at Lookout Creek (26 September). $Q5$ discharge was similar at Sagehen Creek and Coal Creek (0.05 and 0.07 m^3/s , respectively) and about 5 times as high at Lookout Creek (0.26 m^3/s). Similar to RLGW variability, Lookout Creek $Q5$ had lower interannual variability (0.2), while Sagehen and Coal Creeks experienced twice the amount of $Q5$ variability (0.39 and 0.53, respectively). Summer low flow and peak SWE covary, such that years with higher peak SWE have higher summer low flows (Figure 4b). Low-flow discharge was significantly correlated to peak SWE at Sagehen Creek ($R^2 = 0.72, p < 0.01$) and strongly correlated at Coal Creek ($R^2 = 0.48, p = 0.19$), but not significantly correlated at Lookout Creek. Interestingly, at Lookout Creek, summer low flow is less responsive to peak SWE than RLGW proportion (Figure 4c).

3.5. Explaining Low Flows Using Multiple Linear Regression

PCA was leveraged to assess climate differences between the three sites and identify major drivers of RLGW proportion and summer low-flow discharge (Text S3 and Figure S6 in Supporting Information S1). From the scree plot criterion, three PCs were retained above the elbow describing a total of 86% of variance. Variables that were significant on these first three PCs were retained for multiple linear regression. All variables listed in Table 2 were retained, aside from peak SWE day and snow disappearance day.

The degree to which snow and rain parameters explained RLGW proportion varied across the three sites (Figure 5, RLGW columns). The best model fit occurred at Coal Creek ($R^2_{adj} = 0.93$), while Lookout Creek had the weakest fit ($R^2_{adj} = 0.30$). At Coal Creek, melt rate and peak SWE were retained in predicting RLGW, where an increase in melt rate led to an increase in RLGW and an increase in peak SWE led to a decrease in RLGW. Peak SWE was more important (i.e., larger beta weight) than melt rate in predicting RLGW. Sagehen Creek RLGW was predicted with a similar strength as Coal Creek ($R^2_{adj} = 0.92$). At Sagehen Creek, total precipitation and snowfall fraction were retained in predicting RLGW, where an increase in total precipitation and an increase in snowfall fraction led to decreases in RLGW. Total precipitation was twice as important as snowfall fraction suggesting that Sagehen Creek is more precipitation limited than snowfall limited. Lastly, at Lookout Creek, $Q5lag$ was the only variable retained and indicated that years following higher summer flow years had lower RLGW.

Similar to the RLGW proportion models, the best models for predicting $Q5$ (Figure 5, $Q5$ columns) from climate parameters emerged at Sagehen Creek ($R^2_{adj} = 0.85$) and Coal Creek ($R^2_{adj} = 0.74$). At Lookout Creek, no variables were retained in the model indicating that a linear model built with just an intercept and slope of 1 had a lower AIC than any of the snow and rain parameters. At Coal Creek, peak SWE and total precipitation were retained, where total precipitation was nearly twice as important in predicting $Q5$ compared to peak SWE. Increases in total precipitation and decreases in peak SWE led to increases in $Q5$. At Sagehen Creek, total precipitation and SWElag were retained in the model, where an increase in both parameters led to an increase in $Q5$. Total precipitation was over 6 times more important in predicting $Q5$ compared to SWElag.

When we predicted $Q5$ from RLGW (Figure 4c), RLGW was a significant predictor of $Q5$ at all three sites. At Coal Creek, the model performed best ($R^2 = 0.95$) and the Sagehen Creek and Lookout Creek models perform equally ($R^2 = 0.67$). Compared to the snow and rain $Q5$ model, the RLGW $Q5$ model performed better at Lookout Creek and Coal Creek. LOOCV indicated that Lookout Creek models were the most robust (smallest % increase in RMSE), followed closely by Sagehen Creek with Coal Creek models performing the worst (Text S4 and Table S2 in Supporting Information S1).

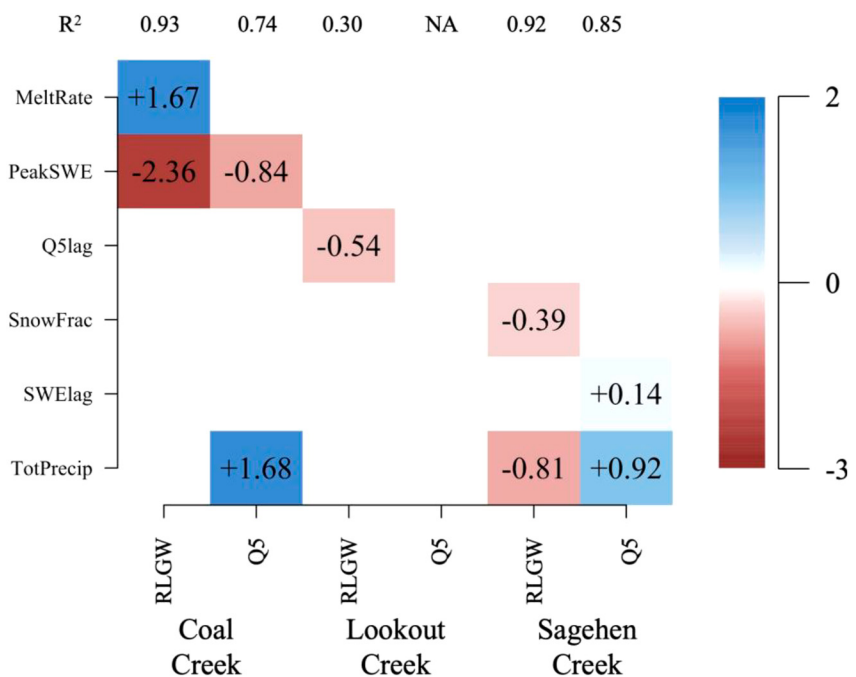


Figure 5. Beta coefficients for models predicting recession limb groundwater (RLGW) and $Q5$ from snow and rain parameters. Darker red indicates more negative beta coefficients, while darker blue indicates more positive beta coefficients. White space indicates that the parameter was not retained in the model. The adjusted R^2 are shown at the top of the plot above the model with which they are associated. See Tables S3–S5 in Supporting Information S1 for p -values, variance inflation factors (VIFs), and beta coefficients for these models.

4. Discussion

Decreases in snow accumulation and earlier melt across the western US driven by a warming climate (Kapnick & Hall, 2012) are causing earlier peak flows and higher reliance on groundwater for summer streamflows. Recent studies attempting to understand the drivers of summer streamflow in the western US have been successful at snow-dominated sites using correlations with snowpack dynamics (Cooper et al., 2018; Godsey et al., 2014). However, sites that have been historically snow dominated are shifting to rain dominated (Klos et al., 2014), leading to a need to focus on understanding drivers of low flow at rain-dominated sites. Here, we build on existing research by examining two behaviors: (a) the controls of recession limb dynamics on the proportion of groundwater delivered to streams and (b) the relationship of summer flows to snow dynamics, RLGW inputs, climate, and flow values from the previous year (i.e., “lagged”). Our results indicate that RLGW proportion is a strong predictor of low flows ($R^2 > 0.65$) at all three sites but is especially important for predicting summer flows in rain-dominated watersheds and that the degree to which RLGW predicts summer low flow may also be mediated by the proportion of dynamic to deep storage. These findings are discussed in detail below.

4.1. Recession Limb Groundwater Reflects Contributions From Dynamic Storage

We introduce RLGW as a metric that can be leveraged to predict $Q5$ across three diverse watersheds. RLGW is the groundwater that contributes to streamflow during the recession limb of the hydrograph and represents groundwater contributions from dynamic storage and deep storage (Figure 6). Dynamic storage is the variation in subsurface storage between dry and wet periods (Dwivedi et al., 2019; Kirchner, 2009; Sayama et al., 2011; Spence, 2007; Staudinger et al., 2017) and has been quantified through storage–discharge relationships (Kirchner, 2009; Sayama et al., 2011), end member mixing (Dwivedi et al., 2019), and streamflow recession analysis (Staudinger et al., 2017). The deep storage zone is the portion of storage that is permanently saturated. We rely on the framework presented by Dwivedi et al. (2019) and utilize two end member mixing to estimate total groundwater contribution during the recession limb. Although RLGW is representative of both dynamic and deep groundwater, interannual variations in RLGW capture variability in dynamic storage

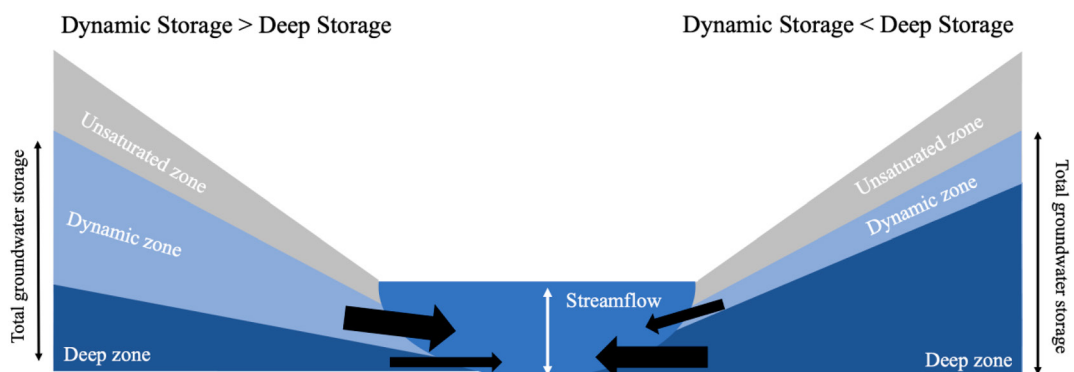


Figure 6. Conceptual model showing three zones that contribute to stream flow (unsaturated, dynamic, and deep zones) during the recession limb for dynamic storage dominated hillslope (left) versus deep storage dominated hillslope (right). Dynamic storage represents the variably saturated portion of the groundwater, while the deep storage represents the permanently saturated portion. All black arrows indicate recession limb groundwater (RLGW) contribution to stream flow.

contributions because contributions from the deep storage zone are relatively constant throughout and across years (Käser & Hunkeler, 2016; Somers et al., 2019). Dynamic storage is recharged during winter and spring precipitation and snowmelt (Dwivedi et al., 2019), but the proportion of dynamic storage in the streamflow during the recession limb is variable. When the proportion of RLGW is low the stream is dominated by runoff (i.e., overland flow, flow through the unsaturated zone) and is less reliant on groundwater for streamflow generation. Therefore, dynamic storage water contributes to streamflow later into the summer. In contrast, when the proportion of RLGW is high, flow is composed of large amounts of dynamic storage water, leading to an earlier draining of the dynamic storage zone, less contribution to late summer flows, and therefore lower low flows (Figure 4c).

4.2. Recession Limb Dynamics Improve Flow Predictions of Summer Low Flows at Rain-Dominated Sites

Estimating summer low flows in snow-dominated watersheds has been done successfully using snow metrics (Cooper et al., 2018; Godsey et al., 2014; Tague & Grant, 2009), but understanding the drivers of summer low flow in rain-dominated and transitional watersheds is challenging. Our work shows that at Lookout Creek and Coal Creek, the RLGW model outperforms the snow and rain metric model. In contrast, the use of RLGW to predict low flow at Sagehen Creek led to weaker model performance (decline in R^2 of 0.18). Although the RLGW model outperforms the climate model at Coal Creek, the climate model still provides strong predictive power of $Q5$ ($R^2_{adj} = 0.74$). In contrast, at Lookout Creek, no climate variables predicted $Q5$, while RLGW led to strong predictive power of $Q5$. Thus, we focus mainly on Lookout Creek as it showed the most improvement in model performance and represents a step forward in low-flow prediction at rain-dominated sites.

The weak relationships between snow parameters and groundwater dynamics (i.e., RLGW and $Q5$) at Lookout Creek suggest that streamflows are less coupled with current year snow and rain parameters compared to Sagehen and Coal Creeks. This is further supported by the low variability in RLGW among years observed at Lookout Creek ($CV = 0.16$ compared to 0.4 and 0.45 at Sagehen and Coal Creeks, respectively). The higher interannual variability at Sagehen Creek and Coal Creek indicates that their RLGW proportions are more responsive to the interannual variation in snowpacks, but the weaker relationship between RLGW and summer low flow compared to the relationship between snow and rain parameters and summer low flow indicates that it is less influential for summer streamflow generation.

Across all three sites, warmer years (i.e., lower SWE, earlier peak SWE dates, and lower snowfall fractions) have higher proportions of RLGW (Figure 4a), which led to lower summer low flows (Figure 4c). These changes are consistent with widespread changes in spring snowpacks occurring across the western US (Mote et al., 2005, 2018; Pederson et al., 2011). The shift from snow-dominated to more rain-dominated suggests that RLGW proportion may become instrumental in predicting summer flows, as demonstrated by the significance of RLGW proportion at Lookout Creek.

4.3. The Degree to Which RLGW Predicts Low Flows Is Mediated by Subsurface Storage

Across all three sites, RLGW is a strong ($R^2 \geq 0.67$) predictor of $Q5$ but improves predictions of $Q5$ at only two sites. Our results suggest that the degree to which RLGW predicts $Q5$ may be mediated by the proportion of dynamic to deep storage. We hypothesize that contributions from the dynamic storage zone control interannual variability in RLGW, but in watersheds where contributions from the dynamic zone are less important in sustaining summer flows (e.g., deep zone $>$ dynamic zone), RLGW is a weaker predictor of $Q5$. In watersheds where the deep zone $>$ dynamic zone, low flows are buffered by water from the deep zone and therefore less sensitive to fluctuations in contributions from the dynamic storage zone (Figure 6).

Residence time can be thought of as a proxy for the proportion of dynamic to deep groundwater storage, where watersheds with a longer mean residence times have a larger proportion of deep storage compared to those with shorter mean residence times. Previous studies at Lookout, Sagehen, and Coal Creeks indicated that Lookout Creek and Coal Creek have short mean residence times in contrast to Sagehen Creek (Hale & McDonnell, 2016; McGuire et al., 2005; Rademacher et al., 2005; Urióstegui et al., 2017). At Lookout Creek, water transit time has been estimated between 0.8 and 3.3 years (McGuire et al., 2005) with an average of 1.8 years (Hale & McDonnell, 2016). At Coal Creek, 20% of annual streamflow is estimated to be contributed from the deep groundwater zone (Zhi et al., 2019), which is similar to the average groundwater proportion we estimate (24%). Other studies in the larger Gunnison River Watershed estimate annual groundwater proportion between 29% (Carroll et al., 2018) and 58% (Miller et al., 2014). These relatively low annual deep groundwater contribution proportions suggest that dynamic storage in Coal Creek exceeds deep storage. Sagehen Creek estimated water ages are much older; Rademacher et al. (2005) estimate that the mean residence time of groundwater feeding Sagehen Creek during baseflow conditions is 28 years. At Lookout and Coal Creeks, RLGW was a stronger predictor than snow and rain parameters (R^2 of 0.67 and 0.95, respectively). Although RLGW shows a similar predictive power at Sagehen Creek as Lookout Creek, it does not perform better than the snow and rain model at Sagehen Creek. This supports our hypothesis that in high dynamic storage systems, spring-season groundwater dynamics are more important in driving summer flows than sites with high deep storage.

In our work, the retention of “lagged” values in the linear models is an indication that there is multiyear storage within a basin. Similar methods have been successfully applied by Brooks et al. (2021) to improve predictions of water yields in snow-dominated watersheds in northern Utah and by Godsey et al. (2014) to improve summer low-flow prediction in the Sierra Nevada. At Lookout Creek, $Q5$ lag emerged as a significant predictor of RLGW and at Sagehen Creek SWElag emerged as a significant predictor of $Q5$. Lagged values were not included in Coal Creek because there are only 5 years of data. The implications of multiyear carryover of low-flow discharges are tightly coupled with climate change. In general, studies have concluded that watersheds with more deep storage are likely to have higher stream flows in the summer but are predicted to experience a larger absolute reduction in summer flows than dynamic storage dominated watersheds, as low-flow discharges compound due to multiyear drought (Mayer & Naman, 2011; Safeeq et al., 2013; Tague & Grant, 2009). Others have found that basins that have large deep storage reservoirs may be buffered from short-term climate impacts (Carlier et al., 2018), that summer low flows will occur earlier but not significantly decline (Godsey et al., 2014), and that although declines in groundwater dominated basins will be larger, declines in surface water-dominated basins will be more damaging to stream habitat (Tague & Grant, 2009). When we consider the potential for streamflow decline at Lookout, Sagehen, and Coal Creeks, literature indicates that Sagehen Creek is more vulnerable to long-term declines in summer streamflow. In contrast, literature suggests that low storage sites such as Lookout and Coal Creeks will be more susceptible to short-term declines in flow (e.g., interannual) but will be more resilient to long-term warming. This is especially true for Lookout Creek, where the watershed is already adapted to rain-dominated climate and thus will likely experience fewer changes in precipitation regime under warming (Safeeq et al., 2013).

4.4. Implications, Limitations, and Future Work

Our work points toward a need to capture RLGW across western US montane watersheds, especially in areas moving toward rain dominance. Large data sets such as the CAMELS-Chem (Sterle et al., 2022), MacroSheds (<https://cuahsi.shinyapps.io/macroshefs/>), or USGS NWIS (<https://nwis.waterdata.usgs.gov/usa/nwis/qwdata>) could offer over 1,000 watersheds across the western US to further explore the importance of RLGW in understanding summer low flows. Overall, the approach used in this work requires few hydrologic parameters, making it scalable to a larger number of basins. Specifically, three main data types are needed: (a) continuous discharge,

(b) discrete stream chemistry, and (c) snow and precipitation data. In montane systems, spatially explicit, high temporal frequency snow depth information is important but challenging to come by over large spatial extents. While SWE reconstruction and spatially distributed SWE models have been developed for areas across the Sierra Nevada (Bair et al., 2016; Dozier, 2011; Rittger et al., 2016) and the Rocky Mountains (Jepsen et al., 2012; Molotch & Margulis, 2008; Molotch et al., 2009), they are inconsistent across different watersheds, and access to those model simulations over the years of particular interest is rare. We leveraged SNODAS data, a 1 km^2 modeled snow product, to calculate snow and rain parameters used in the model. However, point source measurements, such as Natural Resources Conservation Service Snow Telemetry (SNOTEL) stations, would provide similar information. Alternatively, site-specific sources, such as ASO flights (see Figures S1–S3 in Supporting Information S1) or other remotely sensed snow products such as the free, globally available Moderate Resolution Imaging Spectroradiometer (MODIS) Snow and Ice mapping project (snow cover data from 2002 to present at the 500-m scale) could be used. Global precipitation data are available between 1979 and present from the NOAA Global Precipitation Climatology Project (GPCP) Monthly Precipitation Climate Data Record (CDR) data set.

We validated SNODAS snow depth against ASO flights for three dates across Sagehen and Coal Creeks. Overall, SNODAS data showed a slight overprediction (<13%) of snow depth compared to the ASO depths, though over/underprediction at the grid scale (1 km^2) were much larger. This discrepancy between ASO and SNODAS is widely known (Clow et al., 2012; Dozier, 2011; Dozier et al., 2016), although in comparison to other studies, we estimate lower error between ASO and SNODAS. ASO flights are generally concentrated in strongly snow-dominated regions, such as the Sierra and Rocky Mountains, with less focus on transition or rain-dominated watersheds. SNODAS is typically validated against ASO because ground-based observations are assimilated into SNODAS SWE estimation (Oaida et al., 2019). Without more airborne snow data (e.g., ASO flights), SNODAS validation and model improvement are difficult, and the approach employed here appears to be a valid tool to capture average, watershed scale behavior.

Data availability always limits the use of certain models, including the WRTDS model. While guidelines on how long of a record and how frequent chemical parameters must be collected for good model performance are under evaluation (Hirsch & De Cicco, 2015), it does require daily discharge, at least 50 stream chemistry samples spread evenly across the discharge range, and at least 5 years of data. In addition, the model performs best on streams with low intraday variability and is dependent on a strong negative log linear relationship between the chemical parameter of interest and stream discharge, which may not always be the case in some watersheds, especially those impacted by strong anthropogenic activity (Basu et al., 2011; Goldrich-Middaugh et al., 2022; Herndon et al., 2015). Thus, while the model performed well across all three sites (flux bias statistic <0.1, average NSE = 0.90), this may not be the best tool for areas with a dearth of data or highly modified watersheds.

Finally, the last limitation in replicating our approach at other sites is the ability to accurately estimate end members. While we follow guidelines outlined in Miller et al. (2014), end members are derived from measured stream chemistry and rely on representative sampling during both the highest and the lowest flows. High flows are often undersampled (Inamdar & Mitchell, 2006; Murphy et al., 2018; G. P. Williams, 1989) making it difficult to ascertain actual high-flow stream chemistry. However, we assumed that high-flow chemistry is consistent across years and used the entire streamflow record (instead of annual streamflow record) to estimate a high-flow end member, reducing the risk of misrepresenting average high-flow chemistry. Due to a 15+ year period of records at Lookout and Sagehen Creek and high sampling frequency at Coal Creek, this method is reasonable for our sites but is not feasible for sites lacking sufficient data.

Despite limitations to our approach, with robust screening for data availability and consistency, along with additional SWE validation testing, the comparative linear model framework developed in this paper could be widely applied. This is a necessary next step to determine how transferable our conclusions about RLGW are to other locations. Improving prediction methods will provide more accurate information to water managers across the west for better management of summer stream water, when demand for both human and non-human uses are at a maximum. Additionally, low-flow prediction is of interest for understanding water quality (Mosley et al., 2012; Poor & Ullman, 2010), aquatic ecology (Bradford & Heinonen, 2008; Rolls et al., 2012; Stromberg et al., 2007), and sediment transport (Nittrouer et al., 2012) during low-flow conditions. Given that the presented methods performed well in a humid, rain-dominated catchment, RLGW could be used to predict low flows across diverse catchments where low-flow prediction is critical for water management.

5. Conclusion

Understanding factors controlling summer low flow across the western US is critical for low-flow prediction and water allocation. Models often use climate parameters to predict low-flow discharge, and while they consistently perform well at snow-dominated sites, they tend to perform poorly at rain-dominated sites. We used multiple linear regression to compare predictors of low-flow discharge at three sites across the western US spanning snow dominance and varying proportions of dynamic versus deep subsurface storage. We not only leveraged the commonly used suite of climate parameters (e.g., peak SWE, melt rate, and snowfall fraction) but also included lagged hydrodynamics to reflect the influence of previous year snowpack and streamflow. We introduce RLGW as a new metric that provides insight into melt processes through capturing the surface water–groundwater dynamics during melt season. We found that lagged hydrodynamics and RLGW were strong predictors of summer low flow across all three sites and improved predictions of summer low flow at a rain-dominated watershed. Furthermore, the degree to which summer low flow is predicted by RLGW may be mediated by the proportion of dynamic to deep storage. In systems with more dynamic than deep storage, RLGW is likely a better predictor of summer low flow because the stream is more responsive to flow contribution from the dynamic storage zone compared to a deep storage-dominated systems. Overall, what emerges is that including indicators of same year and previous year groundwater dynamics improves low-flow predictions, but the strength of these predictors is tied to subsurface storage. Although we only look at three sites, it is a step toward improving low-flow models. In the future, similar methods could be applied to many sites across the west.

Data Availability Statement

Stream chemistry for Lookout Creek was sourced from the HJ Andrews Experimental Forest Data Catalogue (S. Johnson & Fredriksen, 2019). Stream chemistry for Sagehen Creek was retrieved from USGS NWIS Web (https://waterdata.usgs.gov/usa/nwis/inventory/?site_no=10343500). Stream chemistry for Coal Creek was retrieved from ESS-DIVE (K. Williams et al., 2022). All discharge data were sourced from USGS using the R packages *dataRetreival* and *EGRET* packages (Hirsch & De Ciccio, 2015). For Coal Creek, discharge from USGS gage 09111250 is only operated between 1 April and 15 November. A regression developed from USGS Site ID 385106106571000 was used to estimate continuous daily discharge (Text S1 in Supporting Information S1). SNODAS data are available from NSIDC (NOHRSC, 2004). For related code, please see Zenodo repository (K. Johnson, 2023).

Acknowledgments

This material is based upon work supported by the National Science Foundation under Grants NSF 2034232 and 2012796 (P. L. Sullivan); NSF 2012669 (H. R. Barnard) and the Department of Energy under Grant DE-SC0020146 (P. L. Sullivan).

References

Azmat, M., Liaquat, U. W., Qamar, M. U., & Awan, U. K. (2017). Impacts of changing climate and snow cover on the flow regime of Jhelum River, Western Himalayas. *Regional Environmental Change*, 17(3), 813–825. <https://doi.org/10.1007/s10113-016-1072-6>

Bair, E. H., Ritger, K., Davis, R. E., Painter, T. H., & Dozier, J. (2016). Validating reconstruction of snow water equivalent in California's Sierra Nevada using measurements from the NASA Airborne Snow Observatory. *Water Resources Research*, 52, 8437–8460. <https://doi.org/10.1002/2016WR018704>

Barnhart, T. B., Molotch, N. P., Livneh, B., Harpold, A. A., Knowles, J. F., & Schneider, D. (2016). Snowmelt rate dictates streamflow. *Geophysical Research Letters*, 43, 8006–8016. <https://doi.org/10.1002/2016GL069690>

Barthold, F. K., Tyralla, C., Schneider, K., Vaché, K. B., Frede, H.-G., & Breuer, L. (2011). How many tracers do we need for end member mixing analysis (EMMA)? A sensitivity analysis. *Water Resources Research*, 47, W08519. <https://doi.org/10.1029/2011WR010604>

Barton, K. (2023). MuMIn: Multi-Model Inference. *R package version 1.47.5*. Retrieved from <https://CRAN.R-project.org/package=MuMIn>

Basu, N. B., Thompson, S. E., & Rao, P. S. C. (2011). Hydrologic and biogeochemical functioning of intensively managed catchments: A synthesis of top-down analyses. *Water Resources Research*, 47, W00J15. <https://doi.org/10.1029/2011WR010800>

Bavay, M., Lehming, M., Jonas, T., & Löwe, H. (2009). Simulations of future snow cover and discharge in Alpine headwater catchments. *Hydrological Processes*, 23(1), 95–108. <https://doi.org/10.1002/hyp.7195>

Berghuys, W. R., Woods, R. A., & Hrachowitz, M. (2014). A precipitation shift from snow towards rain leads to a decrease in streamflow. *Nature Climate Change*, 4(7), 583–586. <https://doi.org/10.1038/nclimate2246>

Bernal, S., Butturini, A., & Sabater, F. (2006). Inferring nitrate sources through end member mixing analysis in an intermittent Mediterranean stream. *Biogeochemistry*, 81(3), 269–289. <https://doi.org/10.1007/s10533-006-9041-7>

Blighe, K., & Lun, A. (2022). PCAtools: PCAtools: Everything principal components analysis. *R package version 2.10.0*. Retrieved from <https://github.com/kevinblighe/PCAtools>

Bradford, M. J., & Heinonen, J. S. (2008). Low flows, instream flow needs and fish ecology in small streams. *Canadian Water Resources Journal*, 33(2), 165–180. <https://doi.org/10.4296/cwrij3302165>

Brooks, P. D., Gelderloos, A., Wolf, M. A., Jamison, L. R., Strong, C., Solomon, D. K., et al. (2021). Groundwater-mediated memory of past climate controls water yield in snowmelt-dominated catchments. *Water Resources Research*, 57, e2021WR030605. <https://doi.org/10.1029/2021WR030605>

Carlier, C., Wirth, S. B., Cochand, F., Hunkeler, D., & Brunner, P. (2018). Geology controls streamflow dynamics. *Journal of Hydrology*, 566, 756–769. <https://doi.org/10.1016/j.jhydrol.2018.08.069>

Carroll, R. W. H., Bearup, L. A., Brown, W., Dong, W., Bill, M., & Williams, K. H. (2018). Factors controlling seasonal groundwater and solute flux from snow-dominated basins. *Hydrological Processes*, 32(14), 2187–2202. <https://doi.org/10.1002/hyp.13151>

Clow, D. W., Nanus, L., Verdin, K. L., & Schmidt, J. (2012). Evaluation of SNODAS snow depth and snow water equivalent estimates for the Colorado Rocky Mountains, USA. *Hydrological Processes*, 26(17), 2583–2591. <https://doi.org/10.1002/hyp.9385>

Cooper, M. G., Schaperow, J. R., Cooley, S. W., Alam, S., Smith, L. C., & Lettenmaier, D. P. (2018). Climate elasticity of low flows in the maritime western U.S. mountains. *Water Resources Research*, 54, 5602–5619. <https://doi.org/10.1029/2018WR022816>

Cowie, R. M., Knowles, J. F., Dailey, K. R., Williams, M. W., Mills, T. J., & Molotach, N. P. (2017). Sources of streamflow along a headwater catchment elevational gradient. *Journal of Hydrology*, 549, 163–178. <https://doi.org/10.1016/j.jhydrol.2017.03.044>

Dinpashoh, Y., Singh, V. P., Bazar, S. M., & Kavehkar, S. (2019). Impact of climate change on streamflow timing (case study: Guilan Province). *Theoretical and Applied Climatology*, 138(1), 65–76. <https://doi.org/10.1007/s00704-019-02810-2>

Dozier, J. (2011). Mountain hydrology, snow color, and the fourth paradigm. *Eos, Transactions American Geophysical Union*, 92(43), 373–374. <https://doi.org/10.1029/2011EO430001>

Dozier, J., Bair, E. H., & Davis, R. E. (2016). Estimating the spatial distribution of snow water equivalent in the world's mountains. *WIREs Water*, 3(3), 461–474. <https://doi.org/10.1002/wat2.1140>

Dwivedi, R., Meixner, T., McIntosh, J. C., Ferré, P. A. T., Eastoe, C. J., Niu, G.-Y., et al. (2019). Hydrologic functioning of the deep critical zone and contributions to streamflow in a high-elevation catchment: Testing of multiple conceptual models. *Hydrological Processes*, 33(4), 476–494. <https://doi.org/10.1002/hyp.13363>

Feng, S., & Hu, Q. (2007). Changes in winter snowfall/precipitation ratio in the contiguous United States. *Journal of Geophysical Research*, 112, D15109. <https://doi.org/10.1029/2007JD008397>

Fletcher, T. D. (2022). QuantPsy: Quantitative Psychology tools. *R package version 1.6*. Retrieved from <https://CRAN.R-project.org/package=QuantPsy>

Florianicic, M. G., Bergbuijs, W. R., Molnar, P., & Kirchner, J. W. (2021). Seasonality and drivers of low flows across Europe and the United States. *Water Resources Research*, 57, e2019WR026928. <https://doi.org/10.1029/2019WR026928>

Foks, S. S., Raffensperger, J. P., Penn, C. A., & Driscoll, J. M. (2019). Estimation of base flow by optimal hydrograph separation for the conterminous United States and implications for national-extent hydrologic models. *Water*, 11(8), 1629. <https://doi.org/10.3390/w11081629>

Gaskill, D. L. (1991). Geologic map of the Gothic Quadrangle, Gunnison County, Colorado.

Genereux, D. P., Hemond, H. F., & Mulholland, P. J. (1993). Use of radon-222 and calcium as tracers in a three-end-member mixing model for streamflow generation on the West Fork of Walker Branch Watershed. *Journal of Hydrology*, 142(1), 167–211. [https://doi.org/10.1016/0022-1694\(93\)90010-7](https://doi.org/10.1016/0022-1694(93)90010-7)

Godsey, S. E., Kirchner, J. W., & Tague, C. L. (2014). Effects of changes in winter snowpacks on summer low flows: Case studies in the Sierra Nevada, California, USA. *Hydrological Processes*, 28(19), 5048–5064. <https://doi.org/10.1002/hyp.9943>

Goldrich-Middaugh, G. M., Ma, L., Engle, M. A., Ricketts, J. W., Soto-Montero, P., & Sullivan, P. L. (2022). Regional drivers of stream chemical behavior: Leveraging lithology, land use, and climate gradients across the Colorado River, Texas USA. *Water Resources Research*, 58, e2022WR032155. <https://doi.org/10.1029/2022WR032155>

Gordon, B. L., Brooks, P. D., Krogh, S. A., Boisrame, G. F. S., Carroll, R. W. H., McNamara, J. P., & Harpold, A. A. (2022). Why does snowmelt-driven streamflow response to warming vary? A data-driven review and predictive framework. *Environmental Research Letters*, 17(5), 053004. <https://doi.org/10.1088/1748-9326/ac64b4>

Hale, V. C., & McDonnell, J. J. (2016). Effect of bedrock permeability on stream base flow mean transit time scaling relations: 1. A multiscale catchment intercomparison. *Water Resources Research*, 52, 1358–1374. <https://doi.org/10.1002/2014WR016124>

Harpold, A. A., & Brooks, P. D. (2018). Humidity determines snowpack ablation under warming climate. *Proceedings of the National Academy of Sciences of the United States of America*, 115(6), 1215–1220. <https://doi.org/10.1073/pnas.1716789115>

Herndon, E. M., Dere, A. L., Sullivan, P. L., Norris, D., Reynolds, B., & Brantley, S. L. (2015). Landscape heterogeneity drives contrasting concentration–discharge relationships in shale headwater catchments. *Hydrology and Earth System Sciences*, 19(8), 3333–3347. <https://doi.org/10.5194/hess-19-3333-2015>

Hirsch, R. M., & De Cicco, L. A. (2015). User guide to Exploration and Graphics for RivEr Trends (EGRET) and dataRetrieval: R packages for hydrologic data (version 2.0, February 2015). *U.S. Geological Survey Techniques and Methods* (p. 93). book 4, chap. A10. <https://doi.org/10.3133/tm4A10>

Hirsch, R. M., De Cicco, L. A., & Murphy, J. (2023). Exploration and Graphics for RivEr Trends (EGRET), version 3.0.8. <https://doi.org/10.5066/P9CC9JEX>

Hirsch, R. M., Moyer, D., & Archfield, S. A. (2010). Weighted Regressions on Time, Discharge, and Season (WRTDS), with an application to Chesapeake Bay River inputs. *Journal of the American Water Resources Association*, 46(5), 857–880. <https://doi.org/10.1111/j.1752-1688.2010.00482.x>

Hooper, R. P. (2003). Diagnostic tools for mixing models of stream water chemistry. *Water Resources Research*, 39(3), 1055. <https://doi.org/10.1029/2002WR001528>

Horton, J. D., San Juan, C. A., & Stoeser, D. B. (2017). The State Geologic Map Compilation (SGMC) geodatabase of the conterminous United States (ver. 1.1, August 2017). *U.S. Geological Survey Data Series*, 1052, 46. <https://doi.org/10.3133/ds1052>

Huntington, J. L., & Niswonger, R. G. (2012). Role of surface-water and groundwater interactions on projected summertime streamflow in snow dominated regions: An integrated modeling approach. *Water Resources Research*, 48, W11524. <https://doi.org/10.1029/2012WR012319>

Inamdar, S. P., & Mitchell, M. J. (2006). Hydrologic and topographic controls on storm-event exports of dissolved organic carbon (DOC) and nitrate across catchment scales. *Water Resources Research*, 42, W03421. <https://doi.org/10.1029/2005WR004212>

IPCC. (2022). In H.-O. Pörtner, D. C. Roberts, H. Adams, C. Adler, P. Aldunce, E. Ali, et al. (Eds.), *Climate change 2022: Impacts, adaptation, and vulnerability. Contribution of Working Group II to the Sixth Assessment Report of the Intergovernmental Panel on Climate Change* (p. 3056). Cambridge University Press. <https://doi.org/10.1017/9781009325844>

Jepsen, S. M., Molotach, N. P., Williams, M. W., Rittger, K. E., & Sickman, J. O. (2012). Interannual variability of snowmelt in the Sierra Nevada and Rocky Mountains, United States: Examples from two alpine watersheds. *Water Resources Research*, 48, W02529. <https://doi.org/10.1029/2011WR011006>

Johnson, K. (2023). hydrokeira/Lowflow-WRR: Lowflow prediction analysis code (v1.0) [Software]. Zenodo. <https://doi.org/10.5281/zenodo.7859686>

Johnson, S., & Fredriksen, R. (2019). Stream chemistry concentrations and fluxes using proportional sampling in the Andrews Experimental Forest, 1968 to present. Long-term ecological research [Database]. Forest Science Data Bank. <https://doi.org/10.6073/pasta/bb935444378d112d9189556fd22a441d>

Jones, J. A., & Perkins, R. M. (2010). Extreme flood sensitivity to snow and forest harvest, western Cascades, Oregon, United States. *Water Resources Research*, 46, W12512. <https://doi.org/10.1029/2009WR008632>

Kapnick, S., & Hall, A. (2012). Causes of recent changes in western North American snowpack. *Climate Dynamics*, 38(9–10), 1885–1899. <https://doi.org/10.1007/s00382-011-1089-y>

Käser, D., & Hunkeler, D. (2016). Contribution of alluvial groundwater to the outflow of mountainous catchments. *Water Resources Research*, 52, 680–697. <https://doi.org/10.1002/2014WR016730>

Kirchner, J. W. (2009). Catchments as simple dynamical systems: Catchment characterization, rainfall-runoff modeling, and doing hydrology backward. *Water Resources Research*, 45, W02429. <https://doi.org/10.1029/2008WR006912>

Kish, G. R., Stringer, C. E., Stewart, M. T., Rains, M. C., & Torres, A. E. (2010). A geochemical mass-balance method for base-flow separation, upper Hillsborough River watershed, west-central Florida, 2003–2005 and 2009. *U.S. Geological Survey Scientific Investigations Report 2010-5092* (p. 33).

Klos, P. Z., Link, T. E., & Abatzoglou, J. T. (2014). Extent of the rain–snow transition zone in the western U.S. under historic and projected climate. *Geophysical Research Letters*, 41, 4560–4568. <https://doi.org/10.1002/2014GL060500>

Laaha, G., & Blöschl, G. (2005). Low flow estimates from short stream flow records—A comparison of methods. *Journal of Hydrology*, 306(1), 264–286. <https://doi.org/10.1016/j.jhydrol.2004.09.012>

Mayer, T. D., & Naman, S. W. (2011). Streamflow response to climate as influenced by geology and elevation. *JAWRA Journal of the American Water Resources Association*, 47(4), 724–738. <https://doi.org/10.1111/j.1752-1688.2011.00537.x>

McCreight, J., Dugger, A., RafieeNasab, A., Karsten, L., & Hendricks, A. (2015). rwrhydro: R tools for the WRF Hydro Model. *R package version 1.0.2*.

McGuire, K. J., McDonnell, J. J., Weiler, M., Kendall, C., McGlynn, B. L., Welker, J. M., & Seibert, J. (2005). The role of topography on catchment-scale water residence time. *Water Resources Research*, 41, W05002. <https://doi.org/10.1029/2004WR003657>

Meressa, H., Donegan, S., Golian, S., & Murphy, C. (2022). Simulated changes in seasonal and low flows with climate change for Irish catchments. *Water*, 14(10), 1556. <https://doi.org/10.3390/w14101556>

Miller, M. P., Susong, D. D., Shope, C. L., Heilweil, V. M., & Stolp, B. J. (2014). Continuous estimation of baseflow in snowmelt-dominated streams and rivers in the Upper Colorado River Basin: A chemical hydrograph separation approach. *Water Resources Research*, 50, 6986–6999. <https://doi.org/10.1002/2013WR014939>

Milly, P. C. D., & Dunne, K. A. (2020). Colorado River flow dwindles as warming-driven loss of reflective snow energizes evaporation. *Science*, 367(6483), 1252–1255. <https://doi.org/10.1126/science.aa9187>

Molotch, N. P., Brooks, P. D., Burns, S. P., Litvak, M., Monson, R. K., McConnell, J. R., & Musselman, K. (2009). Ecohydrological controls on snowmelt partitioning in mixed-conifer sub-alpine forests. *Ecohydrology*, 2(2), 129–142. <https://doi.org/10.1002/eco.48>

Molotch, N. P., & Margulis, S. A. (2008). Estimating the distribution of snow water equivalent using remotely sensed snow cover data and a spatially distributed snowmelt model: A multi-resolution, multi-sensor comparison. *Advances in Water Resources*, 31(11), 1503–1514. <https://doi.org/10.1016/j.advwatres.2008.07.017>

Mosley, L. M., Zammit, B., Leyden, E., Heneker, T. M., Hipsey, M. R., Skinner, D., & Aldridge, K. T. (2012). The impact of extreme low flows on the water quality of the lower Murray River and lakes (South Australia). *Water Resources Management*, 26(13), 3923–3946. <https://doi.org/10.1007/s11269-012-0113-2>

Mote, P. W., Hamlet, A. F., Clark, M. P., & Lettenmaier, D. P. (2005). Declining mountain snowpack in western North America. *Bulletin of the American Meteorological Society*, 86(1), 39–50. <https://doi.org/10.1175/BAMS-86-1-39>

Mote, P. W., Li, S., Lettenmaier, D. P., Xiao, M., & Engel, R. (2018). Dramatic declines in snowpack in the western US. *Npj Climate and Atmospheric Science*, 1(1), 2. <https://doi.org/10.1038/s41612-018-0012-1>

Murphy, S. F., McCleskey, R. B., Martin, D. A., Writer, J. H., & Ebel, B. A. (2018). Fire, flood, and drought: Extreme climate events alter flow paths and stream chemistry. *Journal of Geophysical Research: Biogeosciences*, 123, 2513–2526. <https://doi.org/10.1029/2017JG004349>

Musselman, K. N., Addor, N., Vano, J. A., & Molotch, N. P. (2021). Winter melt trends portend widespread declines in snow water resources. *Nature Climate Change*, 11(5), 418–424. <https://doi.org/10.1038/s41558-021-01014-9>

Nash, J. E., & Sutcliffe, J. V. (1970). River flow forecasting through conceptual models part I—A discussion of principles. *Journal of Hydrology*, 10(3), 282–290. [https://doi.org/10.1016/0022-1694\(70\)90255-6](https://doi.org/10.1016/0022-1694(70)90255-6)

National Operational Hydrologic Remote Sensing Center. (2004). Snow Data Assimilation System (SNODAS) Data Products at NSIDC, Version 1 [Dataset]. National Snow and Ice Data Center. <https://doi.org/10.7265/N5TB14TC>

Nittrouer, J. A., Shaw, J., Lamb, M. P., & Mohrig, D. (2012). Spatial and temporal trends for water-flow velocity and bed-material sediment transport in the lower Mississippi River. *GSA Bulletin*, 124(3–4), 400–414. <https://doi.org/10.1130/B30497.1>

Oaida, C. M., Reager, J. T., Andreadis, K. M., David, C. H., Levoe, S. R., Painter, T. H., et al. (2019). A high-resolution data assimilation framework for snow water equivalent estimation across the western United States and validation with the Airborne Snow Observatory. *Journal of Hydrometeorology*, 20(3), 357–378. <https://doi.org/10.1175/JHM-D-18-0009.1>

Painter, T. H., Berisford, D. F., Boardman, J. W., Bormann, K. J., Deems, J. S., Gehrke, F., et al. (2016). The Airborne Snow Observatory: Fusion of scanning lidar, imaging spectrometer, and physically-based modeling for mapping snow water equivalent and snow albedo. *Remote Sensing of Environment*, 184, 139–152. <https://doi.org/10.1016/j.rse.2016.06.018>

Pederson, G. T., Gray, S. T., Ault, T., Marsh, W., Fagre, D. B., Bunn, A. G., et al. (2011). Climatic controls on the snowmelt hydrology of the northern Rocky Mountains. *Journal of Climate*, 24(6), 1666–1687. <https://doi.org/10.1175/2010JCLI3729.1>

Poor, C. J., & Ullman, J. L. (2010). Using regression tree analysis to improve predictions of low-flow nitrate and chloride in Willamette River basin watersheds. *Environmental Management*, 46(5), 771–780. <https://doi.org/10.1007/s00267-010-9550-y>

Poyck, S., Hendrikx, J., McMillan, H., Hreinsson, E., & Woods, R. (2011). Combined snow- and streamflow modelling to estimate impacts of climate change on water resources in the Clutha River, New Zealand. *Journal of Hydrology (NZ)*, 50, 293–312.

Rademacher, L. K., Clark, J. F., Clow, D. W., & Hudson, G. B. (2005). Old groundwater influence on stream hydrochemistry and catchment response times in a small Sierra Nevada catchment: Sagehen Creek, California. *Water Resources Research*, 41, W02004. <https://doi.org/10.1029/2003WR002805>

Rittger, K., Bair, E. H., Kahl, A., & Dozier, J. (2016). Spatial estimates of snow water equivalent from reconstruction. *Advances in Water Resources*, 94, 345–363. <https://doi.org/10.1016/j.advwatres.2016.05.015>

Rolls, R. J., Leigh, C., & Sheldon, F. (2012). Mechanistic effects of low-flow hydrology on riverine ecosystems: Ecological principles and consequences of alteration. *Freshwater Science*, 31(4), 1163–1186. <https://doi.org/10.1899/12-002.1>

Rumsey, C. A., Miller, M. P., Susong, D. D., Tillman, F. D., & Anning, D. W. (2015). Regional scale estimates of baseflow and factors influencing baseflow in the Upper Colorado River Basin. *Journal of Hydrology: Regional Studies*, 4, 91–107. <https://doi.org/10.1016/j.ejrh.2015.04.008>

Safeeq, M., Grant, G. E., Lewis, S. L., & Tague, C. L. (2013). Coupling snowpack and groundwater dynamics to interpret historical streamflow trends in the western United States: Coupling snowpack and groundwater dynamics to interpret streamflow. *Hydrological Processes*, 27(5), 655–668. <https://doi.org/10.1002/hyp.9628>

Sayama, T., McDonnell, J. J., Dhakal, A., & Sullivan, K. (2011). How much water can a watershed store? *Hydrological Processes*, 25(25), 3899–3908. <https://doi.org/10.1002/hyp.8288>

Segura, C., Noone, D., Warren, D., Jones, J. A., Tenny, J., & Ganio, L. M. (2019). Climate, landforms, and geology affect baseflow sources in a mountain catchment. *Water Resources Research*, 55, 5238–5254. <https://doi.org/10.1029/2018WR023551>

Smakhtin, V. U. (2001). Low flow hydrology: A review. *Journal of Hydrology*, 240(3), 147–186. [https://doi.org/10.1016/S0022-1694\(00\)00340-1](https://doi.org/10.1016/S0022-1694(00)00340-1)

Somers, L. D., McKenzie, J. M., Mark, B. G., Lagos, P., Ng, G.-H. C., Wickert, A. D., et al. (2019). Groundwater buffers decreasing glacier melt in an Andean watershed—But not forever. *Geophysical Research Letters*, 46, 13016–13026. <https://doi.org/10.1029/2019GL084730>

Spence, C. (2007). On the relation between dynamic storage and runoff: A discussion on thresholds, efficiency, and function. *Water Resources Research*, 43, W12416. <https://doi.org/10.1029/2006WR005645>

Staudinger, M., Stoezl, M., Seeger, S., Seibert, J., Weiler, M., & Stahl, K. (2017). Catchment water storage variation with elevation. *Hydrological Processes*, 31(11), 2000–2015. <https://doi.org/10.1002/hyp.11158>

Sterle, G., Perdrial, J., Li, L., Adler, T., Underwood, K., Rizzo, D., et al. (2022). CAMELS-Chem: Augmenting CAMELS (Catchment Attributes and Meteorology for Large-sample Studies) with atmospheric and stream water chemistry data. *Hydrology and Earth System Sciences*. Preprint. <https://doi.org/10.5194/hess-2022-81>

Stewart, B., Shanley, J. B., Kirchner, J. W., Norris, D., Adler, T., Bristol, C., et al. (2022). Streams as mirrors: Reading subsurface water chemistry from stream chemistry. *Water Resources Research*, 58, e2021WR029931. <https://doi.org/10.1029/2021WR029931>

Stewart, I. T., Cayan, D. R., & Dettinger, M. D. (2005). Changes toward earlier streamflow timing across western North America. *Journal of Climate*, 18(8), 1136–1155. <https://doi.org/10.1175/JCLI3321.1>

Stewart, M., Cimino, J., & Ross, M. (2007). Calibration of base flow separation methods with streamflow conductivity. *Groundwater*, 45(1), 17–27. <https://doi.org/10.1111/j.1745-6584.2006.00263.x>

Stone, M. (1974). Cross-validatory choice and assessment of statistical predictions. *Journal of the Royal Statistical Society: Series B*, 36(2), 111–133. <https://doi.org/10.1111/j.2517-6161.1974.tb00994.x>

Stromberg, J. C., Beauchamp, V. B., Dixon, M. D., Lite, S. J., & Paradzick, C. (2007). Importance of low-flow and high-flow characteristics to restoration of riparian vegetation along rivers in arid south-western United States. *Freshwater Biology*, 52(4), 651–679. <https://doi.org/10.1111/j.1365-2427.2006.01713.x>

Svensson, C., & Prudhomme, C. (2005). Prediction of British summer river flows using winter predictors. *Theoretical and Applied Climatology*, 82(1–2), 1–15. <https://doi.org/10.1007/s00704-005-0124-5>

Swanson, F. J., & James, M. E. (1975). *Geology and geomorphology of the HJ Andrews Experimental Forest, western Cascades, Oregon*. Res. Pap. PNW-188. US Department of Agriculture, Forest Service, Pacific Northwest Forest and Range Experiment Station.

Tague, C., & Grant, G. E. (2004). A geological framework for interpreting the low-flow regimes of Cascade streams, Willamette River Basin, Oregon. *Water Resources Research*, 40, W04303. <https://doi.org/10.1029/2003WR002629>

Tague, C., & Grant, G. E. (2009). Groundwater dynamics mediate low-flow response to global warming in snow-dominated alpine regions. *Water Resources Research*, 45, W07421. <https://doi.org/10.1029/2008WR007179>

Urióstegui, S. H., Bibby, R. K., Esser, B. K., & Clark, J. F. (2017). Quantifying annual groundwater recharge and storage in the central Sierra Nevada using naturally occurring ^{35}S . *Hydrological Processes*, 31(6), 1382–1397. <https://doi.org/10.1002/hyp.11112>

Vanderbilt, K. L., Lajtha, K., & Swanson, F. J. (2003). Biogeochemistry of unpolluted forested watersheds in the Oregon Cascades: Temporal patterns of precipitation and stream nitrogen fluxes. *Biogeochemistry*, 62(1), 87–117. <https://doi.org/10.1023/A:1021171016945>

Venables, W. N., & Ripley, B. D. (2002). *Modern applied statistics with S* (4th ed.). Springer.

Wang, D., & Cai, X. (2009). Detecting human interferences to low flows through base flow recession analysis. *Water Resources Research*, 45, W07426. <https://doi.org/10.1029/2009WR007819>

Williams, G. P. (1989). Sediment concentration versus water discharge during single hydrologic events in rivers. *Journal of Hydrology*, 111(1–4), 89–106. [https://doi.org/10.1016/0022-1694\(89\)90254-0](https://doi.org/10.1016/0022-1694(89)90254-0)

Williams, K., Dong, W., Brown, W., Carroll, R., & Li, L. (2022). Data from: “Significant stream chemistry response to temperature variations in a high-elevation mountain watershed” [Dataset]. Advancing a Watershed Hydro-Biogeochemical Theory: Linking Water Travel Time and Reaction Rates Under Changing Climate, ESS-DIVE repository. <https://doi.org/10.15485/1892055>

Zambrano-Bigiarini, M. (2020). hydroGOF: Goodness-of-fit functions for comparison of simulated and observed hydrological time series. *R package version 0.4-0*. <https://doi.org/10.5281/zenodo.839854>

Zhi, W., Li, L., Dong, W., Brown, W., Kaye, J., Steefel, C., & Williams, K. H. (2019). Distinct source water chemistry shapes contrasting concentration–discharge patterns. *Water Resources Research*, 55, 4233–4251. <https://doi.org/10.1029/2018WR024257>